

Original Article

# Optimal Allocation of Generation and Reconfiguration of the Distribution Network for Reliability Enhancement using the Mayfly Optimization Algorithm

S. B. Aruna<sup>1</sup>, D. Suchitra<sup>2</sup>

<sup>1,2</sup>Department of Electrical and Electronics Engineering, SRM Institute of Science and Technology, Kattankulathur, Tamilnadu, India.

<sup>1</sup>Corresponding Author : aruna\_ee@hotmail.com

Received: 13 March 2025

Revised: 18 April 2025

Accepted: 30 April 2025

Published: 31 May 2025

**Abstract** - Integrating Distributed Generators (DGs) towards Radial Distribution Networks (RDNs) is currently gaining prominence in power system engineering. This paper describes a recently developed nature-inspired meta-heuristic Mayfly Optimization Algorithm (MOA) for determining the Renewable Energy (RE) based Distribution Generation (DG) integration in Radial Distribution Network (RDN) considering islanding mode and reconfiguration simultaneously. This algorithm provides improved capabilities in choosing the appropriate combination, category, and capacity of renewable energy resources to address the competing needs of the distribution systems. This study claims two major novelties in comparison to the literature. The first is an MOA application that identifies the optimal distribution of Photovoltaic (PV) and Wind Turbine (WT) generation units in RDN when grid-connected mode is used. The second one is the optimum allocation of PV and WT units for supply-demand balance even when islanding occurs, considering reconfiguration options, voltage profile improvement, distribution loss reduction, and optimization of reliability indices. The proposed MOA is able to offer enhanced results in terms of reduction in power losses ~ 57%, Minimum voltage~ 0.96 p.u., and Power index of reliability ~65% when applied with IEEE 33 bus and IEEE 69 bus test systems with various scenarios.

**Keywords** - Distributed generation, Electrical distribution network, Mayfly Optimization Algorithm, Power Index of Reliability, Reliability indices.

## 1. Introduction

Global warming has currently become a major source of concern for all engineering activities around the world. Integrating Renewable Energy Sources (RESs) is one of the feasible alternative possibilities for reducing Green House Gas (GHG) emissions over Conventional Power Plants (CPPs). As a consequence, many countries have established ambitious capacity targets for the installation of RESs in their electrical grids [1]. However, suppose these RESs are not properly installed and scaled. In that case, they can result in problems such as reverse power flows, voltage spikes, and a large increase in electrical network distribution losses. This is especially true for Radial Distribution Networks (RDNs) [2]. Identifying the maximum Hosting Capacity (HC) and enhancing their long-term sustainability and viability is critical in this situation. Integrating RE-based Distribution Generation (DG) into a present-day power system can result in major benefits in distribution networks, including loss minimization, upgrading voltage profile, reliability enhancement, and improvement in power quality[3]. On the other hand, the entire electrical system benefits greatly from

the decrease in dependence on the main grid and consequently from the reduction in power generation from conventional power plants and also the reduction of generation and distribution costs and so forth. In fact, a variety of methods have been employed to achieve these objectives, with loss minimization being a consistent and high-priority operational challenge [4].

Recommended practices include the appropriate integration of Capacitor Banks (CBs)[5] and the implementation of Demand Response (DR) programs and frameworks towards energy management [6, 7]. In addition to these options, Network Reconfiguration (NR) may be the best option, especially when dealing with assuring a reliable and secure power supply by accomplishing operational objectives [8, 9]. A large number of researchers have addressed the Optimal Sharing of Distribution Generation (OADG) problem by using a variety of Analytical Approaches (AAs)[10] as well as Heuristic Approaches(HAs) in this area[11]. Harris Hawks Optimizer(HHO) and its upgraded version, Improved Harris Hawks Optimizer (IHHO), are presented for resolving the



OADG Problem as a particular objective function for power loss reduction [12]. A modified Sine Cosine Algorithm (MSCA) is adopted for the OADG problem, with an emphasis on Ploss, Fast Voltage Stability Index (FVSI), and overall costs, with DG dispersion level [13]. Order of Preference using Similarity to Ideal Solution (TOPSIA) technique and Monarch Butterfly Optimization (MBO) were combined to create an innovative hybrid method for curtailing the annual energy loss and RE fluctuations [14, 15]. The integration of several types of DGs was optimized using the Manta Ray Foraging Optimization method (MRFO) in order to maximize the electrical distribution network performance [16].

A Chaotic Salp Swarm Algorithm (CSSA) with multiple fuzzy rules was used for addressing PV in addition to Battery Energy Storage System (BESS) allocation in EDNs [17, 18]. Whale Optimization Algorithm (WOA) seeks to regulate the optimum DG position and size in the distribution system [19, 20]. In [21], Loss Sensitivity Factors (LSF), fuzzy rules, and Sine Cosine Algorithm (SCA) were employed in a hybrid technique to solve the OADG problem with Ploss minimization. A unique hybrid approach combining the IHHO algorithm as well as Particle Swarm Optimization (PSO) is implemented to enhance the incorporation of renewable sources into network operation for technical paybacks [22, 23]. Distributed generation sources are located and configured on radial distribution networks; the Genetic Moth Swarm Algorithm (GMSA) aims to minimize electrical power loss [24, 25].

For deterministic and dynamic OADG problems incorporating load uncertainty for DISCO profit maximization, the harmony search algorithm (HSA) and the Firefly Algorithm (FA) have been integrated. On the other side, the OADG problem is also solved simultaneously by considering Optimal Network Reconfiguration (ONR) [26, 27]. To curtail voltage deviation and real power loss, the Multi-Verse Optimization (MVO) algorithm was implemented in IEEE radial power distribution systems [28]. To mitigate real power loss, the Flower Pollination Algorithm (FPA) was used in IEEE radial distribution test systems [29]. Using a hybrid analytical simulation method, the reliability evaluation of a microgrid with organized loads and dispersed RES was presented [30]. Based on literature reviews of [31, 32], it is obvious that the RDN's performance may be considerably enriched in terms of the benefits to society, the economy, and the environment. A new metaheuristic method for solving optimisation problems in radial distribution networks, the Mayfly Optimisation Algorithm (MOA), is presented in this research. The distinctiveness of the MOA technique is that it attempts to greatly enhance distribution network performance by integrating the OADG and ONR problems, in contrast to methods that handle these issues independently, as revealed by the findings of the literature survey. The major contributions made by this research study are outlined below:

- To propose the Mayfly optimization algorithm for the preeminent approach to distributing PV and wind-founded DGs to the IEEE 33 and 69 bus systems in order to boost the voltage profile and limit distribution losses in both grid-connected and islanded scenarios.
- Under grid-associated and Islanded modes of operation, a measure has been taken to analyse the different reliability indices such as SAIDI, SAIFI, CAIDI, ASAI, and ASUI.
- To show the effectiveness of the Mayfly Optimization algorithm, the Cuckoo Search Algorithm (CSA), Particle Swarm Optimisation (PSO), Grasshopper Optimisation Algorithm (GOA), and Flower Pollination Algorithm (FPA), and outcomes were compared. In contrast to techniques that address both difficulties independently, the strategy aims to improve distribution network performance significantly by addressing the OADG and ONR problems.

Following the introduction in Section 1, the current research study is systematically arranged as follows. Section 2 focuses on the mathematical modeling of RESs, optimization problem formulation, and the relevant constraints. Section 3 explores the theoretical notion of MOA in terms of mathematical relations and the technique for implementing it. Section 4 delves into the simulation results of different scenarios on IEEE 33-bus RDNs and IEEE 69-bus RDNs utilizing the suggested technique, while Section 5 summarizes the research study's overall key conclusions.

## 2. Modeling of Renewable Sources of Energy and Problem Formulation

This section provides mathematical modeling of various kinds of DGs that have been incorporated in load flow. In addition, the operating modes of grid-connected and islanding modes and the assumptions included in this work are associated with handling the load flow. Among the many RESs, Wind Turbines (WT) and solar Photovoltaic (PV) electricity sources are the main contributors. PVs generate DC power, which is then fed into the grid using DC/AC converters. When these converters' operating power factors are considered, PV sources can be seen as perfect actual power providers. WTs on the other hand, may be suitable for reactive power injection if their power converters' operating power factor control can be changed to satisfy the reactive power injection need. As a result, for both PV and WT sources, the following mathematical relationships are introduced to compensate for real and reactive power loads:

$$P'_{d(k)} = P_{d(k)} - P_{res(k)} \quad (1)$$

$$Q'_{d(k)} = Q_{d(k)} - P_{res(k)} \times \tan(\text{pf}_{(k)}) \quad (2)$$

Where  $P'_{d(k)}$  and  $Q'_{d(k)}$  were the net real as well as reactive power loads at bus- $k$  after integrating RES at bus- $k$ ;  $pf_{(k)}$  is the operating power factor of the RES's converter, which can be unity for PV, and it is variable for WT systems.

## 2.1. Network Operational Modes

### 2.1.1. Normal Mode

The real power and total reactive power load shortage need to be acquired from the main grid if only solar PV-type DGs are integrated. In the case of reactive power type DGs like Capacitor Banks (CBs) integration, the overall real power load and the deficit in reactive power load are expected to be imported by the main grid. In the case of integrating WT-based DGs, the deficiency in both active in addition to reactive power is impermissibly imported from the main grid. When the network operational condition is addressed by means of the load flow technique [34], the sub-station bus is handled as a slack bus with p.u., and appropriate deficit load and losses are allocated to it from the main grid, which is then imported into the network.

### 2.1.2. Islanding Mode

Under this mode, the required real and reactive power loads are supposed to be supplied by only DGs in the network. In this stage, the DG sizes and locations are chosen at random and optimized during the optimization process by considering the Slack bus, which is associated with the largest DG among all with p.u.

Under grid-connected mode, the DGs' capacity may not be equivalent to the entire network load; the deficit power and distribution losses, can be treated as the real power demand not being met by DGs when the network is under islanding conditions. In this case, the DG allocation problem is intended to optimize not only network performance but also reliability without violating any operational constraints.

## 2.2. Objective Functions

The mathematical models are described as follows :

### 2.2.1. Power Index of Reliability

The Power Index of Reliability (  $PIR$  ) is defined in this study using total real power demand (i.e., load + losses) of the network in grid-connected mode (  $P_D$  ) and real power demand that the DGs do not meet under islanding conditions (  $P'_D$  ); it is given by,

$$PIR = 1 - \frac{P'_D}{P_D} \quad (3)$$

The value of  $PIR$  becomes 1 if the network is able to supply total  $P_D$  since  $P'_D$  is zero. Similarly, the value of  $PIR$  can also become 0 if the network is not able to supply the total  $P_D$  and thus  $P'_D$  is equal to  $P_D$ .

### 2.2.2. Voltage Deviation Index

Keeping the voltage profile constant throughout the network is vital. The variation from a reference voltage is known as the Voltage Deviation Index (VDI), and it is provided by the equation,

$$VDI = \frac{1}{nb} \times \sum_{n=1}^{nb} \sqrt{\left( |V_{(ref)}| - |V_{(n)}| \right)^2} \quad (4)$$

### 2.2.3. Real Power Distribution Losses

The overall distribution losses of a network are estimated by adding the ohmic losses of all of its branches using the formula,

$$P_{loss} = \sum_{k=1}^{nbr} I_{k(ij)}^2 r_{k(ij)} \quad (5)$$

Where  $r_{k(ij)}$  is the resistance and  $I_{k(ij)}$  is the current magnitude through a branch- $k$  connected amongst buses  $i$  and  $j$ ;  $P_{loss}$  is the total distribution losses and  $nbr$  is the total number of branches in the network. The overall multi-objective function used by  $PIR$ ,  $VDI$ , and  $P_{loss}$  is now defined as follows

$$f_{ov} = \min (PIR + VDI + P_{loss}) \quad (6)$$

### 2.2.4. Planning and Operational Constraints

The solution to the suggested multi-objective function stated in Equation (6) is found to take into account the following planning and operational constraints:

Bus voltage constraint:

$$|V_{(i),min}| \leq |V_{(i)}| \leq |V_{(i),max}|; \quad \forall i = 1 \dots nb \quad (7)$$

Branch thermal limit:

$$S_{(k)} \leq S_{(k),max}; \quad \forall k = 1 \dots nbr \quad (8)$$

Network radiality constraint:

$$nbr = nb - 1 \quad \& \quad \det(\bar{A}) = 0 \quad (9)$$

DG real power capacity limit:

$$P_{G,res} = \sum_{k=1}^{ndg} P_{res(k)} \leq \sum_{i=1}^{nbus} P_{d(i)} \quad (10)$$

DG reactive power capacity limit:

$$Q_{G,res} = \sum_{k=1}^{ndg} Q_{res(k)} \leq \sum_{i=1}^{nbus} Q_{d(i)} \quad (11)$$

Where  $|V_{(i)}|$ ,  $|V_{(i),\max}|$  and  $|V_{(i),\min}|$  are voltage magnitude of bus-i, maximum and minimum limits;  $P_{G, \text{res}}$  and  $P_{\text{res}(k)}$  are the total real power generation by RES DGs and at a DG at bus-k;  $Q_{G, \text{res}}$  and  $Q_{\text{res}(k)}$  are the overall reactive power generation by entirely RES DGs and at a DG at bus-k;  $S_{(k)}$  and  $S_{(k),\max}$  are the power flow in a branch-k and its maximum boundary;  $nb$  and  $ndg$  are related to total buses and DGs in the system;  $\bar{A}$  is bus-incident matrix.

### 3. Mayfly Optimization Algorithm

In 2020, Zervoudakis K et al. created Mayfly Optimization Algorithm (MOA) to promote reproducing behaviour in mayflies [35]. They belong to the ancient insect order Paleoptera and are members of the Ephemeroptera group. The MOA is a nature-inspired meta-heuristic algorithm with high efficiency that has been shown to improve problem-solving performance. MOA is a hybrid algorithm because it combines elements from PSO, GA, and FA. The MOA method and the sequential stages needed to solve the proposed optimisation problem are explained mathematically in this section.

#### 3.1. Modeling of Mayfly Optimization Algorithm

At the primary level, MOA, like altogether population exploration algorithms, generates arbitrary search spaces for a set of male mayflies that make up the solution candidates. Likewise, the location vector for all search agents is provided by  $X = [x_1, x_2, \dots, x_D]^T$ ,  $x_{i,\min} \leq \forall x_i \leq x_{i,\max}$ . Through assessment of the primary position vector presentation relative to the suggested objective function  $f_{ov}$  defined in Equation (6), it is probable to define the velocity vector  $V = [v_1, v_2, \dots, v_D]^T$ , which, depending on their combined and individual search experiences, will be utilized to update the mayflies' location within the search area.

##### 3.1.1. Characterization of Stochastic Behaviour in Male Mayflies

Based on their individual fitness, the search agents move to a new location ( $x_{\text{best}}$ ), and Then, among the entire mayflies, the position that is assessed to be appropriate ( $x_{g,\text{best}}$ ) is handled. For the subsequent level, the new location of male mayflies  $x_i(k+1)$  is resolute by means of its present location  $x_i(k)$  and restructured velocity for the subsequent step  $v_i(k+1)$ , based on the relationship that follows, which is taken into consideration:

$$x_i(k+1) = v_i(k+1) + x_i(k) \quad (12)$$

At a height of several meters, the algorithm affords the male mayflies a steady speed as they continue their nuptial dance and is calculated using the subsequent formula,

$$v_{id}(k+1) = v_{id}(k) + c_1 \times \exp(-\zeta D_x^2) \times [x_{id,\text{best}}(k) - x_{id}(k)] + c_2 \times \exp(-\zeta D_g^2) \times [x_{id,\text{gbest}}(k) - x_{id}(k)] \quad (13)$$

Where  $c_1$  and  $c_2$  are the two positive aspects that scale the ratio of social and cognitive factors;  $\zeta$  diminishes mayfly prominence in relation to one another,  $D_x$  and  $D_g$  are the spaces amongst  $x_{id}$  and  $x_{id,\text{best}}$ ,  $x_{id}$  and  $x_{id,\text{gbest}}$ ,  $v_{id}(k)$  and  $v_{id}(k+1)$  are the  $i$ th mayfly's  $d$ -dimensional velocity regarding present as well as upcoming iterations, respectively.

$$\|D_x\| = \sqrt{\sum_{j=1}^D (x_{ij} - X_{ij})^2} \quad (14)$$

Where  $x_{ij}$  is the  $j$ th element of  $i$ th mayfly and  $X_{ij}$  relates to either  $x_{id,\text{best}}$  and  $x_{id,\text{gbest}}$ .

For the minimization problem, the local best as well as global best populations  $x_{id,\text{best}}$  and  $x_{id,\text{gbest}}$  for the current iteration are computed by,

$$x_{id,\text{best}} = \begin{cases} x_{id}(k+1) & \text{if } f_{ov}(x_{id}(k+1)) < f_{ov}(x_{id,\text{best}}) \\ x_{id,\text{best}} & \text{else} \end{cases} \quad (15)$$

$$x_{id,\text{gbest}} = \min\{f_{ov}(x_{id,\text{best}}) \forall i \in D\} \quad (16)$$

For the swarm of mayflies to successfully mate, they must continue to exhibit their unique nuptial dance characteristics. This shows their oscillatory movements by,

$$v_{id}(k+1) = v_{id}(k) + n_d \times r_i \quad (17)$$

Where  $n_d$  represents the nuptial dance constant and  $r_i$  is an arbitrary variable amongst  $[-1, 1]$ . The algorithm's stochastic behaviour is provided by this dance feature.

##### 3.1.2. Evaluation of Female Mayflies Stochastic Behaviour

Female mayflies don't create swarms when they migrate to male mayflies for breeding as male mayflies do. Let  $y_{id}(k)$  be a female  $i$ th mayfly's current location in the search space of dimension  $d$ ,  $y_{i,\min} \leq \forall y_i \leq y_{i,\max}$ , its position is restructured to the present situation and is provided by,

$$y_i(k+1) = v_i(k+1) + y_i(k) \quad (18)$$

In the current iteration, the attraction is now treated as deterministic rather than arbitrary by considering that the reproducing procedure among the first best male and first female mayflies, the second best male and second female mayflies, and so forth is its fitness function. The female mayflies' velocities for this mating are updated by

$$v_{ij}(k+1) = \begin{cases} v_{ij}(k) + c_3 \times \exp(-\zeta D_{mf}^2) \times [x_{ij}(k) - y_{ij}(k)] & \text{if } f_{ov}(y_i(k)) > f_{ov}(x_i(k)) \\ v_{ij}(k) + fl * r_j & \text{if } f_{ov}(y_i(k)) \leq f_{ov}(x_i(k)) \end{cases} \quad (19)$$

Where  $v_{ij}(k)$  is  $i$ th female mayfly velocity in feature  $j = 1:D$  at existing iteration  $k$ ;  $y_{ij}(k)$  is the present position of  $i$ th female mayfly in aspect  $j$ ;  $c_3$  is positive attraction constant, and  $D_{mf}$  is the Cartesian distance amongst male

and female mayflies which can be determined by Equation (14),  $fl$  and  $r_j$  are a random variable between  $[-1, 1]$ , respectively, and the arbitrary walk for female mayflies that are drawn to male mayflies.

### 3.1.3. Characterization of the Mating Process

By using a crossover operator of GA, Male and female mayflies have a streamlined mating process. According to their positions in the swarm and their fitness functions. The outcomes of the crossover are two offspring, as produced by,

$$\begin{aligned} OS_1 &= R * M_p + (1-R) * F_p \quad \text{and} \\ OS_2 &= R * F_p + (1-R) * M_p \end{aligned} \quad (20)$$

Here,  $M_p$  and  $F_p$  are the male and female parents,  $R$  is a random number amongst specified range and  $OS$  are the two offspring by initial values are zero.

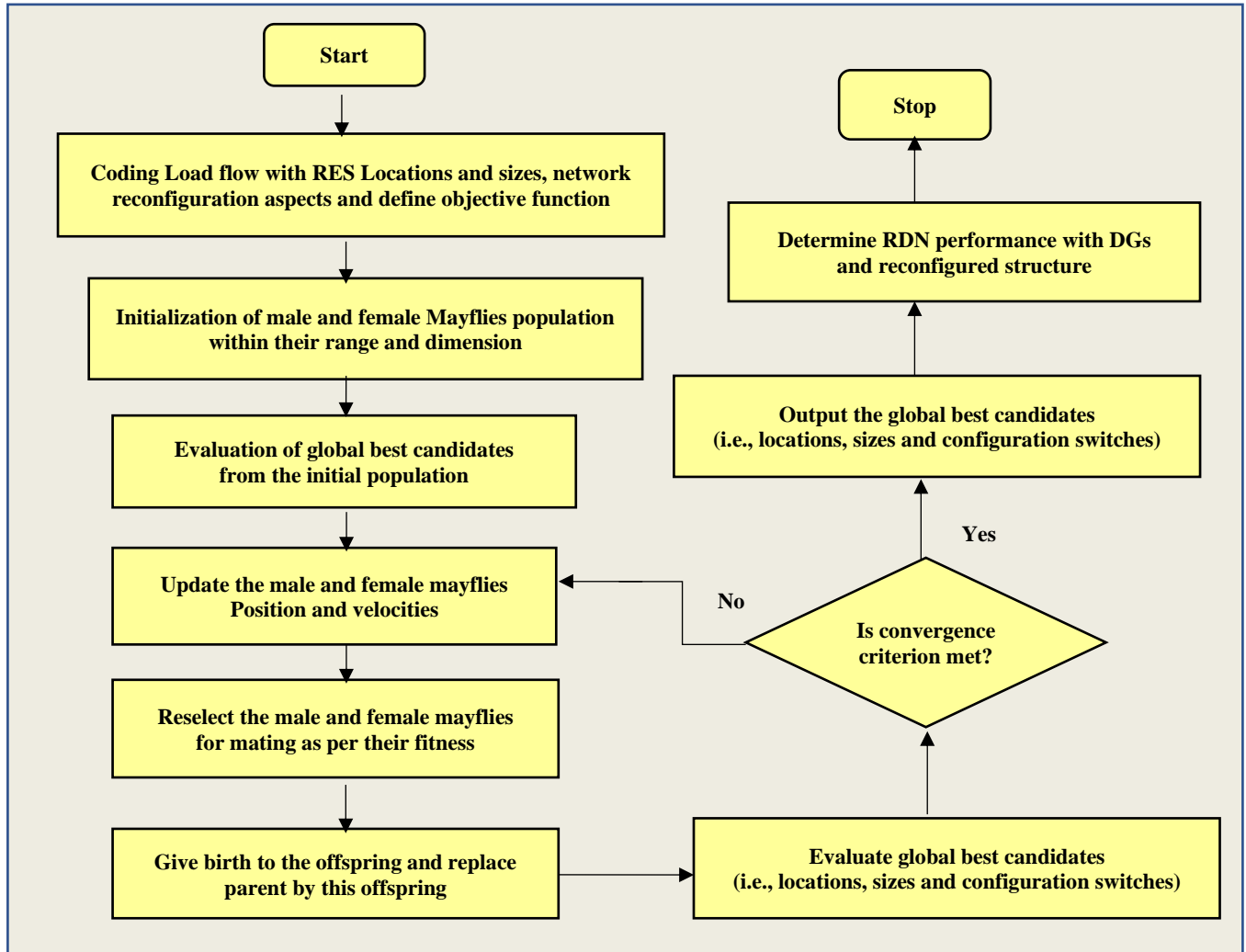


Fig. 1 Implementation of proposed MOA for solving OADG problem and ONR problem

### 3.2. Solution Methodology

The Mayfly algorithm combines the benefits of PSO, FA, and GA algorithms to provide better exploration capability, prominent solution accuracy, and rapid convergence. It differs from PSO as it integrates gender-based duties with male and female mayflies using distinct movement methods, but it persists in applying velocity and location updates to coordinate the search agents (mayflies) within the solution space. Reproduction and mutation are adopted from GA by MOA, although they are enhanced via attraction-based mating as opposed to random crossover. It employs distance-dependent attraction to manage exploration and exploitation, similar to FA, but it models it differently between opposing genders. These characteristics make MOA a potent tool for resolving challenging, nonlinear optimisation issues by better balancing local refinement and global search. Due to its high computation accuracy and simple structure, researchers use it to address issues in a wide range of disciplines. The implementation procedure of the proposed MOA for resolving the OADG and ONR problems is given in Figure 1.

- Step 1: Initialize the population for the DG locations randomly between buses  $[2, nb]$ , the sizes between  $[0, P_d/ndg]$ , and the switch numbers to open in the initial closed structure between  $[1, nbr + ntie]$ .
- Step 2: Check for the radiality constraint by determining the number of loops ( $nl$ ) and the number of sub-graphs ( $ng$ ) from the newly generated graph, considering random switches that open in the network. Check for the convergence of load flow with the DGs and determine the fitness function for the initial population.
- Step 3: From the fitness of the initial population, determine the global best and update male female mayflies' positions and velocities and perform the mating process as described in the process of MOA.
- Step 4: Determine the global best candidate solutions after reaching the convergence criteria (i.e., when  $k = k_{max}$ ). Determine the performance with DG and reconfigured structure.
- Step 5: Compare the results with the literature works.

## 4. Results and Discussion

The Mayfly algorithm is used in this work to integrate dispersed renewable energy generation for the distribution system in the best possible way to give consumers reliable power [35]. The proposed methodology distinguishes itself by concurrently addressing DG allocation and network reconfiguration using the Mayfly Algorithm. This dual-focus strategy aims to minimize power losses, improve voltage stability, and enhance overall system reliability. By integrating both optimization problems, the approach seeks to achieve better enhancement of distribution network performance compared to methods that treat these issues

separately. The IEEE 33-bus test system and IEEE 69-bus test system are considered in the simulations. Four scenarios are investigated for both systems in order to determine the computational efficiency of the suggested MOA in solving the optimum incorporation of distributed renewable energy generation. By using Mayfly algorithm, optimization problem is handled by considering parameters such as maximum iterations = 50, population size (male and Female Mayflies) = 20, Inertia Weight Damping Ratio = 1, Individual Learning Coefficient  $a_1 = 1.0$ , Inertia weight = 0.8, Global Learning Coefficients  $a_2 = 1.5$  and  $a_3 = 1.5$ , Number of Offsprings = 2, positive attraction constants for velocity control  $c_1 = 1.0$  and  $c_2 = 1.5$ . These parameters collectively ensured effective convergence toward the ideal size and location of distributed generation units. In contrast to other population-based techniques, this leads to an overall computational complexity of about, showing a moderate computational impact that is efficient while maintaining effective optimisation for DG unit placement and sizing.

The simulations are done on a PC with Windows 10 Pro 64-bit Intel Pentium CPU N3540 @2.16GHz, 4GB RAM using MATLAB programming. Each test system is analyzed by taking the grid-connected mode in Scenario 1, and the optimal sharing of three solar PV systems is determined. Scenario 2 determines the optimal distribution of three wind turbine systems while taking grid mode into account. Scenarios 3 and 4 solve the optimal sharing of three solar PV systems and the optimal allocation of three wind turbine systems in islanding mode with reconfiguration.

The multi-objective function in Scenarios 1 and 2 seeks to improve network performance by lowering distribution losses and improving voltage profiles. Power index reliability (PIR), voltage profile improvement, distribution loss lessening, and reliability enhancement are all considered in Scenarios 3 and 4.

Furthermore, reliability indices comprising System Average Interruption Frequency Index (SAIFI) (f/c.yr), Customer Average Interruption Duration Index (CAIDI) (hr/c.int), System Average Interruption Duration Index (SAIDI) (hr/c.yr), Average Service Unavailability Index (ASUI) (p.u.) and Average Service Availability Index (ASAI) (p.u.) are determined for the whole network by using the data of failure rate (f/yr) and repair time (h) [36, 37].

### 4.1. Performance Assessment and Reliability Indices of IEEE 33 – Bus Test System

The test system contains 33 buses linked by 32 sectionalizers/branches and 5 tie-lines, as shown in Figure 2, to serve a whole load of (3715 kW + j 2300 kVar). When all tie-lines are opened under this loading condition, the total loss is (210.9983 kW + j 143.0329 kVar), and the voltage deviation index (VDI) is 0.0111. Further, bus -18 appears to have the lowest voltage magnitude at 0.9038 p.u.

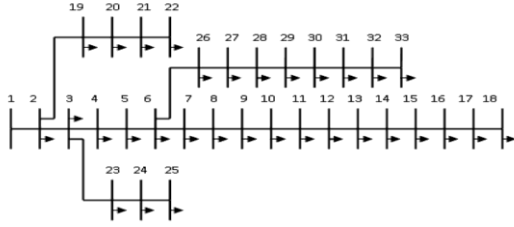


Fig. 2 Single-line IEEE 33-bus test system representation

As DG power is not available and the complete load disconnects under islanding conditions, PIR is zero in this situation. This scenario will be used as the base case operating condition for future discussions. Reliability indices of the IEEE 33 - bus test system without any DG source, i.e., base case, are determined as follows: SAIFI = 2.5894 (f/c.yr), SAIDI = 2.2990 (hr/c.yr), CAIDI = 0.8879 (hr/c.int), ASAI = 0.9997 (p.u.) and ASUI = 0.00025 (p.u.).

#### 4.1.1. Scenario 1: Optimal distribution of three solar PV systems in grid-connected mode.

The optimal solar PV systems will be integrated with the main grid at three optimal sites for the purpose of voltage profile enhancement and decreasing total distribution losses.

Solar PV systems only offer real power, and their capacity may not be enough to fulfill the network's entire real power load; thus, any shortages, along with total network distribution losses and reactive power load, are provided by the main grid. Under islanding conditions, the deficit actual power and total distribution losses are equal to the total unmet demand.

As a result, the PIR may be lower, indicating network reliability. From the analysis, the optimal findings obtained by MOA are noted to be as follows: buses 13, 24, and 30 are in optimal positions, whereas the ideal sizes in kW are 800.956, 1090.97, and 1054.01, respectively. The real power losses are observed as 72.787 kW, and the VDI is lowered to 0.00373, associated with the base case values.

In Table 1, the outcomes of MOA are contrasted to those of literature studies. According to this comparison, the results achieved by MOA are superior to those obtained by MBO [14], MOWOA [16], WOA [20], and SCA [21]. The reliability indices of this scenario are calculated as: SAIFI=2.5741(f/c.yr), SAIDI= 2.2791(hr/c.yr), CAIDI = 0.8854 (hr/c.int), ASAI = 0.9997 (p.u.) ,ASUI = 0.00026 (p.u.) .

Table 1. Optimal allocation of three solar PV systems in IEEE 33-bus considering grid-connected mode and comparison with literature.

Algorithm	Optimal PV Sizes (kW)(bus)	$P_{loss}$ (kW)	$Q_{loss}$ (kVAr)	VDI	$ V_{min} $ (p.u.)( bus)
MBO [14]	754(14),1099(24), 1071(30)	72.806	50.706	0.00378	0.9686(33)
MOWOA[16]	1021.6(14),1200 (24), 1200(31)	81.069	57.745	0.00215	0.9810(33)
WOA [20]	1072.83(30),772.49 (25), 856.68 (13)	73.757	51.010	0.00363	0.9688(33)
SCA [21]	805.71(13), 1104.32(24), 1044.23(30)	72.791	50.651	0.00372	0.9685(33)
MOA	1090.97(24),800.96 (13), 1054.01(30)	72.787	50.654	0.00373	0.9687(33)

Now, the network has been re-evaluated, considering islanding mode. When an upstream defect or other disruption causes a distribution system to separate electrically from the power system as an entire system. Yet powered by the DG connected to it, this condition is known as islanding. The system's inherent issues or load changes that go above permitted thresholds could also contribute to islanding.

According to the load flow, the maximum PV system's bus is treated as a slack bus when determining network performance, as presented in Table 2. As previously stated, the required reactive power demand must be met locally; therefore, the kVAr generation at the slack bus is converted to the

appropriate STATCOM capacity for network stability management in islanding mode and to adjust the voltage at the moment of connection to a distribution system. As can be seen, MOWOA [16] has a higher PIR because of the higher installed DG capacity. Through power factor improvement and voltage stability enhancement under fluctuating load, STATCOM offsets reactive power demand. The amount of demand that is not met by DGs under islanding mode is given as  $P_D'$ . As a result, the DGs allocation problem must be re-evaluated in the context of islanding mode, and ONR can be explored for further improvement. These are the basic motivations for Scenarios 3 and 4 in this work, respectively.

Table 2. Evaluation of IEEE 33-bus test system performance considering optimal PV systems under islanding mode.

Algorithm	$P_{G,res}$ (kW)	$P_D'$ (kW)	STATCOM (kVAr)	PIR	$P_{loss}$ (kW)	VDI	$ V_{min} $ (p.u.) (bus)
MBO [14]	2924.00	889.174	2374.14	0.7607	98.174	0.0064	0.9521(33)
MOWOA[16]	3421.60	394.126	2376.69	0.8939	100.726	0.0046	0.9663( 29)
WOA [20]	2702.00	1119.076	2380.48	0.6988	106.072	0.0088	0.9326 (22)
SCA [21]	2954.26	858.488	2373.74	0.7689	97.747	0.0064	0.9521 (33)
MOA	2945.94	866.726	2373.69	0.7667	97.662	0.0064	0.9242(33)

#### 4.1.2. Scenario 2: Optimal Allocation of Three WT Systems in Grid-Connected Mode

The optimal WT systems, with operating power factors ranging from 0.3 to 0.95 [38], will be integrated with the main grid at three optimal sites to reduce overall distribution losses and voltage profile. As a result of this analysis, using MOA, the following optimal findings are obtained: the optimal sites are buses 13, 24, and 30, and the optimal sizes in kW/pf are 789.30/0.9, 1068.30/0.9 and 1037.52/0.72, respectively. When compared to the base case values, the real power losses are reduced to 11.749kW, and the VDI is reduced to 0.00076.

As WT systems can support both real and reactive power, they can provide better performance than PV systems. The outcomes of MOA are compared to those of previous literature studies in the same Table 3. According to this comparison, MOA's results are superior to those obtained by BSOA [39], BFOA [40], and IHHO [12]. The respective reliability indices are SAIFI = 2.5741 (f/c.yr), SAIDI = 2.2791(hr/c.yr), CAIDI = 0.8854 (hr/c.int), ASAI = 0.9997 (p.u.) and ASUI = 0.00026 (p.u.). The network performance is re-evaluated in the islanding mode, and the findings are shown in Table 4.

**Table 3. Optimal allocation of 3 WT systems in IEEE 33-bus system in grid-associated mode**

Algorithm	WT Systems(kW/pf) (bus)	$P_{loss}$ (kW)	$Q_{loss}$ (kVAr)	VDI	$ V_{min} $ (p.u.) (bus)
BSOA[39]	698/0.86 (13),402/0.71 (29),658/0.70 (31)	29.648	21.201	0.00173	0.9795(25)
BFOA[40]	600/0.89 (14),598/0.83 (25),934/0.88 (30)	27.189	19.339	0.00299	0.9759(33)
HHO [12]	913.05/0.85(12),882.86/0.82(24),1079.05/0.83(30)	15.104	11.846	0.00076	0.9914(18)
IHHO [12]	761.82/0.90(12),1141.92/0.91(24),1013.83/0.71 (30)	13.079	10.890	0.00139	0.9814(18)
MOA	1068.30/0.9(24),789.30/0.9(13), 1037.52/0.72(30)	11.749	9.763	0.00076	0.9922(8)

**Table 4. Evaluation of IEEE 33-bus system performance WT systems under islanding mode**

Algorithm	$P_{G,res}$ (kW)	$P_D$ (kW)	STATCOM (kVAr)	PIR	$P_{loss}$ (kW)	VDI	$ V_{min} $ (p.u.) (bus)
BSOA[39]	1758.00	2268.49	1048.38	0.3894	311.488	0.01921	0.8413(25)
BFO [40]	2132.00	1674.86	1156.42	0.5492	91.858	0.00823	0.9360 (22)
HHO [12]	2874.96	885.03	426.96	0.7618	44.986	0.00461	0.9592 (22)
IHHO [12]	2917.57	822.29	425.08	0.7787	24.860	0.00311	0.9706 (18)
MOA	2895.12	842.57	418.43	0.7732	22.686	0.00247	0.9807 (22)

#### 4.1.3. Scenario 3: Optimal Allocation of Three Solar PV Systems Considering Islanding and Reconfiguration

The optimal sizes of PV systems are integrated in this scenario to meet total network demand even under islanding conditions. To ensure high PIR with minimal distribution losses, the optimal network reconfiguration based on branch exchange type is also carried out concurrently. By opening sectionalizing switches (which are often closed) and securing tie switches (which are typically open) of the network, a network reconfiguration technique is implemented. When a feeder partition fails, this method primarily aids the network in restoring power and reducing feeder overloads by instantaneously shifting the load to nearby feeders. In contrast to Scenarios 1 and 2, the load flow considers the maximum PV system's bus as a slack bus when determining network performance. As mentioned earlier, the required reactive power demand is to be supplied locally; thus, the kVAr generation at the slack bus is made equivalent to the required STATCOM capacity for managing network stability under islanding mode. The optimal results of MOA are as follows: buses 3, 15, and 30 are the best places, according to Table 5, and the best kW sizes are 967.51, 720.02, and 882.03, respectively. The tie-line 25-29(s37) is still open in the ideal arrangement, while the others 8-21(s33), 9-15(s34), 12-

22(s35) and 18-33(s36) are closed. The sectionalizers 7-8(s7), 9-10(s9), 14-15(s14), and 32-33(s33) are, on the other hand, opened. The network performance is as follows:  $P_{loss}$  = 56.440 kW; VDI = 0.00302, PIR = 0.6765, and  $V_{min}$  = 0.9694 (14). At this stage, the total RES capacity is 2569.59 kW, and there is a requirement for BESS to be around 1201.88 kW. Further, BESS provides voltage regulation and frequency support for the network. In addition, the network has no reactive power sources. Hence, the needed STATCOM/CB is 2344.962 kVAr. The reliability indices are as follows: SAIFI = 2.5719 (f/c.yr), SAIDI = 1.7114 (hr/c.yr), CAIDI = 0.6654 (hr/c.int), ASAI = 0.9998 (p.u.) and ASUI = 0.00021 (p.u.). To associate the computational effectiveness of the suggested MOA, different algorithms such as the Cuckoo Search Algorithm (CSA), Flower Pollination Algorithm (FPA), Grasshopper Optimization Algorithm (GOA), and Particle Swarm Optimization (PSO), performance characteristics taken from literature and MOA are simulated for 50 independent runs, and the results are shown in the same Table 5. Performance matrices, such as worst, best, mode, mean, median, and standard deviation, are also provided, and it is perceived that the suggested MOA overtakes other algorithms in terms of low best, mode, mean, and median values and the convergence characteristics are given in Figure 3.



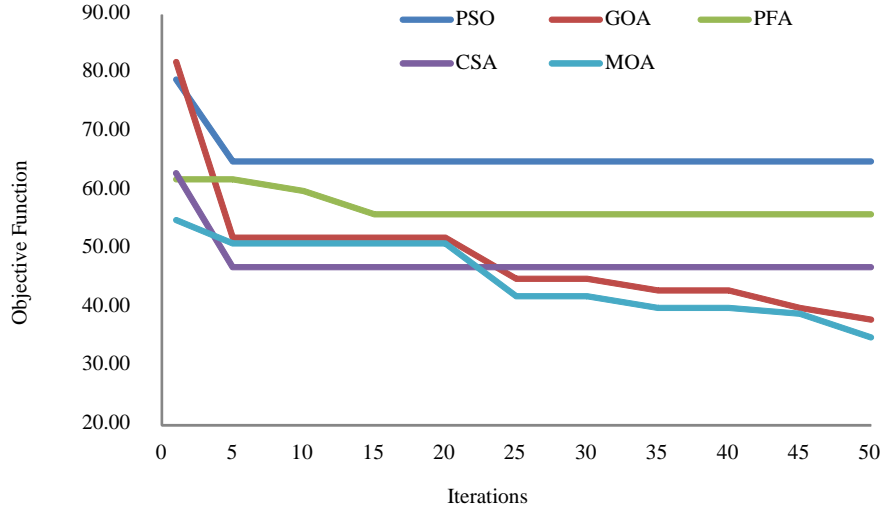


Fig. 3 Convergence characteristics of various algorithms while solving Scenario 3 in IEEE 33-bus RDN

Table 5. Optimal allocation of three PV systems in IEEE 33-bus system considering islanding and reconfiguration

Algorithm	PSO[4-6]	FPA[29]	CSA[4-6]	GOA[4-6]	MOA
PV Systems (kW)	828.84 (30)	924.22(22)	593.00(26)	672.96(31)	882.03(30)
	870.66(23)	437.20 (32)	667.89(15)	697.50 (15)	720.02(15)
	701.95 (9)	1085.51(3)	851.20 (3)	895.87 (3)	967.51 (3)
$P_{G,res}$	2401.45	2446.93	2112.10	2266.33	2569.56
BESS (kW)	1382.45	1331.47	1671.07	1506.30	1201.88
STATCOM/CB(kVAr)	2353.413	2350.545	2353.772	2345.652	2349.62
$P_{loss}$	68.895	63.404	68.171	57.628	56.440
VDI	0.00452	0.00395	0.00383	0.00323	0.00302
PIR	0.6279	0.6416	0.5502	0.5945	0.6765
$V_{min}$	0.9615 (14)	0.9603 (33)	0.9585 (32)	0.9691 (14)	0.9694 (14)
Best	69.527	64.049	58.226	68.725	57.119
Worst	92.442	84.528	<b>78.029</b>	95.225	78.976
Mode	70.740	65.117	58.226	68.725	57.119
Mean	72.579	67.366	62.728	71.060	59.757
Median	70.695	65.117	62.495	68.725	57.267
Std	<b>5.033</b>	6.108	5.190	7.022	5.834

The Mayfly Optimisation Algorithm (MOA) performed better than the compared algorithms. It demonstrated greater operating efficiency by achieving the lowest real power loss (56.44 kW) and the lowest loss per unit (0.00302). Additionally, MOA produced the highest minimum voltage (0.9694 p.u.) and voltage Deviation index (0.6765), both of which are essential for maintaining grid stability and avoiding under-voltage problems.

#### 4.1.4. Scenario 4: Optimal Allocation of three WT Systems Considering Islanding and Reconfiguration

A similar procedure of Scenario 3 is followed for defining the optimal WT locations and sizes in this case. According to Table 6, the best MOA results are as follows: buses 3, 8, and 30 are the best places, and the best kW sizes along with their optimal pf are 909.419/ 0.313, 837.09/0.882

and 716.026/0.586, respectively. Notably, the best configuration obtained in Scenario 3 still remains the same. Consequently, the network performance is as follows:  $P_{loss}$  = 25.128 kW; VDI = 0.00195, PIR = 0.6561, and  $V_{min}$  = 0.9779 (14). In addition to the total RES capacity of 2462.54 kW, 1277.6 kW of BESS capacity is required.

Furthermore, because the network lacks reactive power sources, the required STATCOM/CB is 1875.59 kVAr under capacitive mode. Reliability indices are as follows: SAIFI = 2.5719 (f/c.yr), SAIDI = 1.7114 (hr/c.yr), CAIDI = 0.6654 (hr/c.int), ASAI = 0.9998 (p.u.) and ASUI = 0.00021 (p.u.). The performances of MOA in comparison with other algorithms are also provided in Table 6; convergence characteristics are displayed in Figure 4.

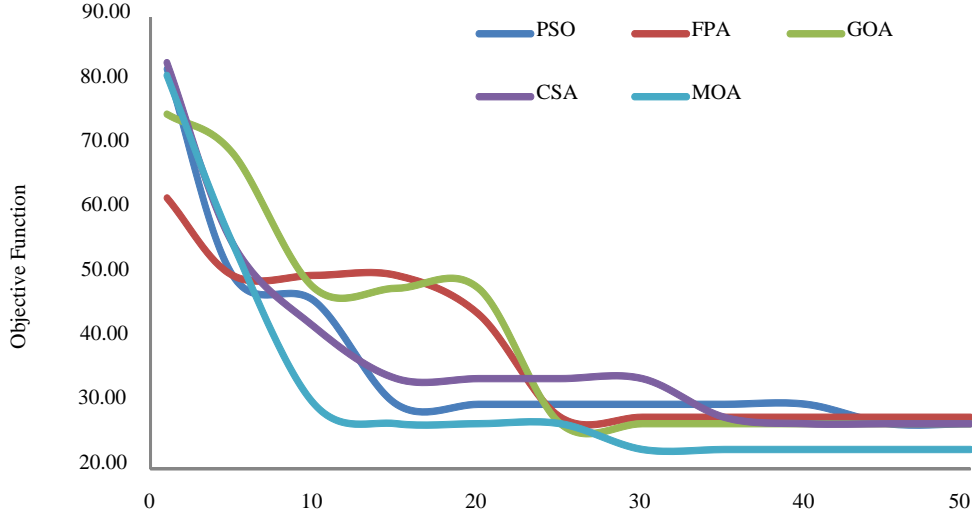


Fig. 4 Convergence characteristics of different algorithms while solving Scenario 4 in IEEE 33-bus RDN

Table 6. Optimal allocation of three WT systems in IEEE 33-bus system considering islanding and reconfiguration

Algorithm	PSO[4-6]	FPA[29]	CSA[4-6]	GOA[4-6]	MOA
WT systems (kW/bus/pf)	936.655/23/0.643 892.114/21/0.803 891.058/30/0.762	847.837/30/0.672 659.92 /16/0.896 1018.140/30/0.948	778.889/8/0.796 708.289/30/0.607 1006.431/30/0.640	906.194/3/0.861 639.498/15/0.885 674.087/30/0.597	909.419/3/0.313 837.090/8/0.88 716.026/30/0.586
$P_{G,res}$	2719.83	2525.91	2493.61	2219.78	2462.54
BESS (kW)	1024.1	1216.2	1247.6	1523.1	1277.6
STATCOM/CB(kVAr)	209.82	719.76	405.64	545.88	1875.59
<b>PIR</b>	0.7243	0.6726	0.6642	0.5900	0.6561
$P_{loss}$	28.947	27.143	26.177	27.920	25.128
<b>VDI</b>	0.00293	0.00199	0.00183	0.00213	0.00195
$ V_{min} $	0.9656 (33)	0.9732 (14)	0.9790 (14)	0.9730 (14)	0.9779 (14)
Best	29.67	27.82	26.84	28.51	25.79
Worst	79.09	61.63	72.82	82.61	81.98
Mode	32.13	27.82	45.62	30.83	25.84
Mean	36.74	34.67	39.03	35.23	30.07
Median	32.13	27.82	31.42	30.83	25.84
Std	12.15	9.38	12.61	12.30	11.24

When integrating wind turbine systems with BESS and STATCOM components, the MOA-based technique once more performs better than competing algorithms. The MOA achieves the lowest real power loss (25.128 kW), demonstrating that it guarantees effective energy distribution even though it does not achieve the lowest total WT installation capacity (2462.54 kW compared to PSO's 2719.83 kW).

#### 4.2. Performance Assessment and Reliability Indices of IEEE 69-bus system

The test system contains 69 buses [38] linked by 68 sectionalizer / branches and 5 tie-lines shown in Figure 5 to serve a total load (3802.10 kW + j 2694.70 kVAr). When all tie-lines are opened under this loading condition, it has a whole loss of (225.0007 kW + j 102.1648 kVAr) and a Voltage

Deviation Index (VDI) of 0.0046 as well, and bus-65 has the lowest voltage magnitude of 0.9092 p.u. PIR is zero in this condition due to the absence of DG power and the whole load disconnecting under islanding conditions.

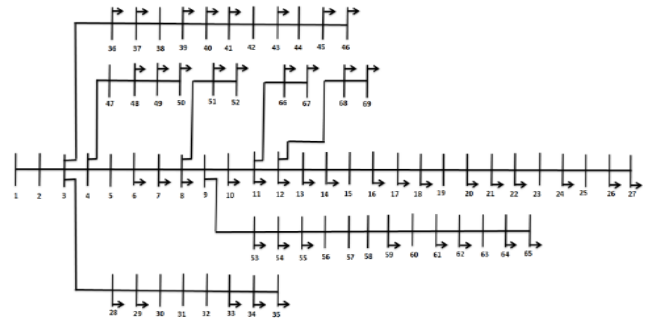


Fig. 5 Single-line illustration of IEEE 69-bus test system

Reliability indices of this case are as follows: SAIFI = 1.8874(f/c. yr), SAIDI=1.2091(hr/c. yr), CAIDI = 0.6692(hr/c.int) , ASAI = 0.9999 (p.u.) and ASUI = 0.00014 (p.u.).

#### 4.2.1. Scenario 1: Optimal Allocation of Three Solar PV Systems in Grid-Connected Mode

Three solar PV systems are integrated into the system based on the optimal findings achieved by MOA as follows: the optimal positions are buses 11, 17, and 61, and the optimal sizes in kW are 526.67, 380.53, and 1718.98, respectively.

The real power loss is observed to be 69.429 kW, and the VDI is lowered to 0.00105 compared to the base case values. In Table 7, the outcomes of MOA are compared to those of previous literature studies. According to this comparison, the results achieved by MOA are superior to those obtained by WOA [20], SCA [21], HHO-PSO [22], and GMSA [24]. Also, the lowermost voltage magnitude is observed at bus-65 as 0.9790 p.u. The reliability indices are calculated as SAIFI = 1.8174 (f/c.yr), SAIDI = 1.2054 (hr/c.yr), CAIDI = 0.6638 (hr/c.int), ASAI = 0.9998 (p.u.) and ASUI = 0.00012 (p.u.). IEEE 69-bus test system performance considering optimal PV systems under islanding mode is presented in Table 8.

**Table 7. Optimal allocation of three solar PV systems in IEEE 69-bus considering grid-connected mode**

Algorithm	Optimal PV Sizes (kW)(bus)	$P_{loss}$ (kW)	$Q_{loss}$ (kVAr)	VDI	$ V_{min} $ (p.u.)( bus)
WOA [20]	489.02 (11), 476.48 (18), 1680.30 (61)	69.756	35.063	0.00099	0.9780(65)
SCA [21]	522.22 (11), 396.24(18), 1711.40 (61)	69.438	34.963	0.00104	0.9788 (65)
HHO-PSO[22]	571.70 (11), 366.90 (18), 1701.80 (61)	69.450	34.963	0.00106	0.9786(65)
GMSA [24]	526.00 (11), 380.70 (17), 1718.00 (61)	69.430	34.963	0.00105	0.9789(65)
MOA	526.67 (11), 380.53 (17), 1718.98 (61)	69.429	34.962	0.00105	0.9790 (65)

**Table 8. Evaluation of IEEE 69-bus test system performance considering optimal PV systems under islanding mode**

Algorithm	$P_{G,res}$ (kW)	$P_D$ (kW)	STATCOM (kVAr)	PIR	$P_{loss}$ (kW)	VDI	$ V_{min} $ (p.u.) (bus)
WOA[20]	2645.80	1156.30	2694.70	0.696	141.595	0.00667	0.9302(65)
SCA [21]	2629.86	1172.24	2694.70	0.692	145.262	0.00690	0.9287(65)
HHO-PSO [22]	2640.40	1161.70	2694.70	0.694	143.534	0.00685	0.9293(65)
GMSA [24]	2624.70	1177.40	2694.70	0.690	146.279	0.00696	0.9283 (65)
MOA	2626.17	1175.93	2694.70	0.691	146.235	0.00695	0.9283 (65)

#### 4.2.2. Scenario 2: Optimal Allocation of Three WT Systems in Grid-Connected Mode

The optimal findings of MOA for incorporating WT systems are: the optimal positions are buses 13, 24, and 30, whereas the optimal sizes in kW/pf are 498.63/0.821(11), 376.25/0.828 (18), 1686.92/0.823 (61) respectively. When related to the base case values, the real power loss is minimised to 4.285 kW, and VDI is reduced to 0.00076. The

outcomes of MOA are compared to those of literature studies in Tables 9 and 10. According to this comparison, MOA's results are superior to those achieved by WOA [20], SCA [21], HHO-PSO [22], and GMSA [24]. The reliability indices are SAIFI=1.8174 (f/c.yr), SAIDI=1.2054 (hr/c.yr), CAIDI=0.6639 (hr/c.int), ASAI =0.9998 (p.u.), ASUI=0.00012 (p.u).

**Table 9. Optimal allocation of 3 WT systems in IEEE 69-bus system in grid-associated mode**

Algorithm	WT Systems(kW/pf) (bus)	$P_{loss}$ (kW)	$Q_{loss}$ (kVAr)	VDI	$ V_{min} $ (p.u.) (bus)
WOA[20]	498.6/0.82(11), 376.2/0.82(18), 1686.9/0.82(61)	4.285	6.766	0.00016	0.9943(50)
SCA [21]	693.4/0.88(11), 281.33/0.78(21), 1580.52/0.83(61)	5.651	7.335	0.00032	0.9921 (65)
HHO-PSO[22]	406.56/0.82(11), 309.7/0.83(18), 1422.9/0.81(61)	8.721	8.850	0.00076	0.9848 (65)
GMSA[24]	409.63/0.83(11), 311.21/0.82(18), 1413.23/0.81(61)	9.120	9.026	0.00077	0.9843 (65)
MOA	420.6 /0.8(11), 302.9/0.85(17), 1418.99 /0.81(61)	8.826	8.878	0.00077	0.9847 (65)

**Table 10. Evaluation of IEEE 69-bus system considering optimal WT systems under islanding mode**

Algorithm	$P_{G,res}$ (kW)	$P_D$ (kW)	STATCOM (kVar)	PIR	$P_{loss}$ (kW)	VDI	$ V_{min} $ (p.u.) (bus)
WOA[20]	2555.25	1246.85	1070.17	0.672	88.961	0.00577	0.9383 (50)
SCA [21]	2139.26	1662.85	1172.58	0.563	118.235	0.00690	0.9390 (50)
HHO-PSO [22]	2134.07	1668.03	1193.55	0.561	117.965	0.00689	0.9290 (50)
GMSA [24]	2142.52	1659.58	1164.18	0.564	116.857	0.00687	0.9388 (50)
MOA	2561.70	1240.40	913.47	0.674	96.130	0.00608	0.9354 (50)

#### 4.2.3. Scenario 3: Optimal Allocation of Three Solar PV Systems Considering Islanding and Reconfiguration

The optimal results of MOA are as follows: buses 49, 61, and 21 are the best places, according to Table 11, and the best kW sizes are 1403.42, 1334.64, and 767.93, respectively. The tie-line 11-43(s69) and 13-21(s70) are still open in the optimal reconfiguration, while the others 15-46(s71), 50-59(s72), and 27-65(s73) are closed. The sectionalizer 14-15(s15), 57-58(s57) and 61-62(s61) are, on the other hand opened. The performance of the network is as follows:  $P_{loss} = 38.408$  kW;

VDI = 0.00183, PIR = 0.912, and  $V_{min} = 0.9728$  (62). At this stage, the total RES capacity is 3505.99 kW, and there is a requirement for BESS to be around 334.52 kW. In addition, the network has no reactive power sources. Hence, the needed STATCOM/CB is 2733.82 kVar. The respective reliability indices are as follows: SAIFI = 1.5959 (f/c.yr), SAIDI = 1.2384 (hr/c.yr), CAIDI = 0.776 (hr/c.int), ASAI = 0.9998 (p.u.) and ASUI = 0.00012 (p.u.). The MOA performance in comparison with other algorithms is also provided in Table 11. and convergence characteristics are presented in Figure 6.

**Table 11. Optimal allocation of three PV systems in IEEE 69-bus system considering islanding and reconfiguration**

Algorithm	PSO[4-6]	GOA[4-6]	FPA[29]	CSA[4-6]	MOA
PV Systems (kW)	1065.73 (61) 1734.99 (39) 446.62 (38)	711.68 (26) 1078.43(61) 1630.75(49)	1101.91 (8) 1360.91 (49) 648.76 (61)	1738.93(36) 1561.52(60) 540.42 (27)	1403.42(49) 1334.64(61) 767.93(21)
$P_{G,res}$	3247.35	3420.87	3111.58	3840.87	3505.99
BESS (kW)	619.27	420.94	746.79	623.05	334.52
STATCOM/CB(kVAR)	2770.34	2735.78	2749.88	2740.67	2733.82
$P_{loss}$	64.510	39.707	56.272	44.820	38.408
VDI	0.00224	0.00180	0.00259	0.00120	0.00183
PIR	0.8371	0.8893	0.8036	0.9984	0.912
$ V_{min} $	0.9599 (61)	0.9785 (62)	0.9541 (62)	0.9724 (61)	0.9728 (62)
Best	64.510	39.707	56.272	44.820	38.408
Worst	77.810	81.212	62.465	63.086	54.211
Mode	64.510	52.394	56.272	44.820	52.982
Mean	65.099	48.392	57.474	45.186	47.010
Median	64.510	46.676	56.272	44.820	44.523
Std	7.726	2.652	6.126	2.583	2.310

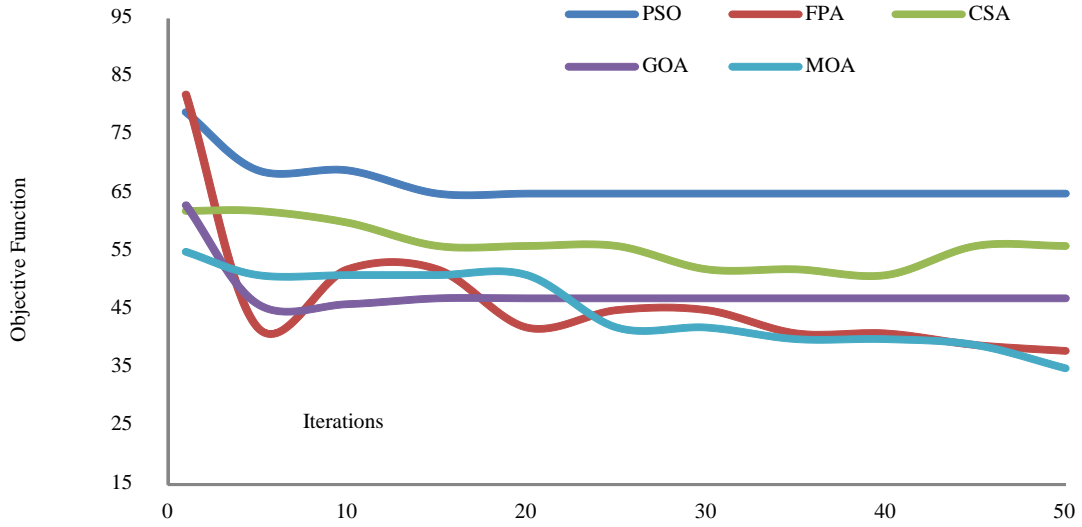


Fig. 6 Convergence features of various algorithms while solving scenario 3 in IEEE 69 - bus RDN

The Mayfly Optimisation Algorithm (MOA) outperforms more conventional techniques like PSO and FPA, producing the lowest real power loss (38.408 kW). MOA maintains a higher level of consistency, as evidenced by its lowest standard deviation (2.310), whereas CSA displays a little better p.u. loss and voltage deviation index.

#### 4.2.4. Scenario 4: Optimal Allocation of three WT Systems Considering Islanding and Reconfiguration

According to Table 12, the best MOA results are as follows: buses 61, 48, and 27 are the best places, and the best kW sizes along with their optimal pf are 1085.15/0.689, 1217.85/0.921 and 494.29/0.78, respectively. Notably,

the best configuration, as obtained in Scenario 3, is still the same. The performance of the network is as follows:  $P_{\text{loss}} = 14.246$  kW,  $VDI = 0.00078$ ,  $PIR = 0.732$ , and  $V_{\text{min}} = 0.9883$  (69). In addition to the total RES capacity of 2797.292, 1019.054 kW of BESS capacity is required. Furthermore, because the network lacks reactive power sources, the required STATCOM/CB is 656.115 kVAr. The respective reliability indices are as follows: SAIFI = 1.5959 (f/c.yr), SAIDI = 1.2384 (hr/c.yr), CAIDI = 0.776 (hr/c.int), ASAI = 0.9998 (p.u.) and ASUI = 0.00012 (p.u.). The performance of MOA in comparison with other algorithms is also provided in Table 12, and the convergence aspects are shown in Figure 7.

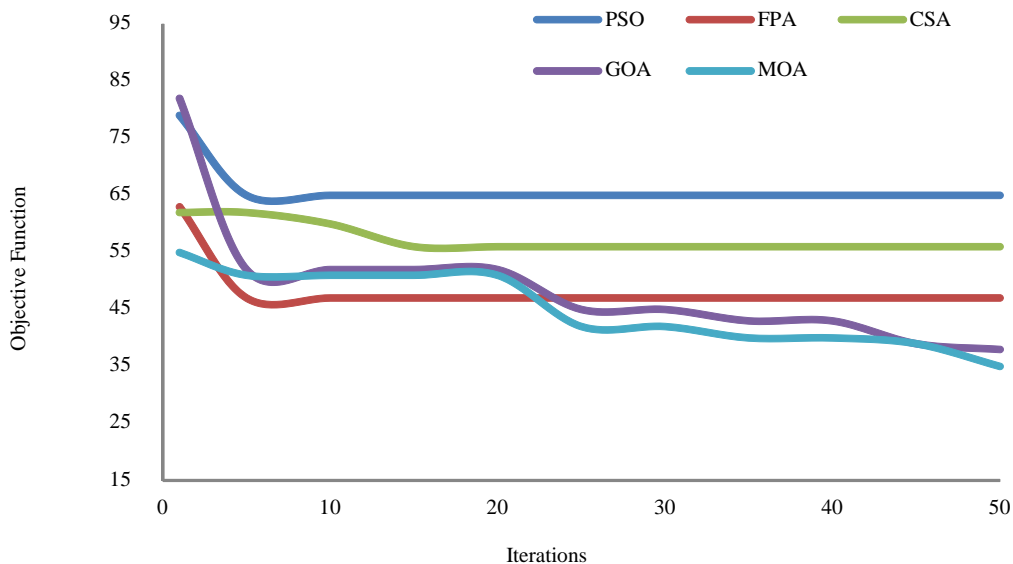


Fig. 7 Convergence features of different algorithms while solving Scenario 4 in IEEE 69-bus RDN

**Table 12. Optimal allocation of three WT systems in IEEE 69-bus system considering islanding and reconfiguration**

Algorithm	PSO[4-6]	FPA[29]	CSA[4-6]	GOA[4-6]	MOA
WT Systems (kW/bus/pf)	964.61/ 61/ 0.999 930.30/ 47/ 0.512 799.73/ 24/ 0.923	1027.43/ 45/ 0.886 1336.27/ 36/ 0.749 1341.98/ 61/ 0.733	1552.4/ 49/ 0.488 890.68/ 61/ 0.687 508.68/ 26/ 0.750	929.62/ 49/ 0.722 581.03/ 27/ 0.799 892.64/ 61/ 0.661	1085.15/ 61/ 0.689 1217.85/ 48/ 0.921 494.29/ 27/ 0.780
$P_{G,res}$	2694.638	3705.683	2951.767	2403.279	2797.292
BESS (kW)	1131.125kW	117.527kW	867.968kW	1415.903kW	1019.054kW
STATCOM/ CB(kVAr)	781.078 kVAr	-253.25 kVAr	-1449.467 kVAr	370.743 kVAr	656.115 kVAr
$P_{loss}$	23.663	21.11	17.635	17.082	14.246
VDI	0.0013	0.00083	0.00131	0.00124	0.00078
PIR	0.702	0.969	0.772	0.628	0.732
$ V_{min} $	0.9823 (69)	0.9803 (62)	0.9829 (69)	0.983 (69)	0.9883 (69)
Best	23.663	21.110	17.635	17.082	<b>14.246</b>
Worst	46.620	51.758	41.899	31.709	<b>29.361</b>
Mode	24.772	26.814	26.301	31.709	<b>18.222</b>
Mean	31.403	24.133	24.127	<b>20.537</b>	21.644
Median	31.958	21.860	24.712	18.502	<b>18.222</b>
Std	6.461	9.463	4.611	4.936	<b>3.107</b>

MOA achieved the lowest real power losses (14.246 kW) and lowest loss per unit (0.00078), indicating high operational efficiency and superior performance with other algorithms. Furthermore, MOA presented the highest minimum voltage (0.9883 p.u.), suggesting tremendous voltage stability across the network. While FPA had the highest total WT capacity (3705.683 kW), MOA maintained a more balanced system with optimal BESS sizing and minimal reactive power compensation, enhancing system reliability.

#### 4.3. Summary

The performance enhancement aspects and reliability analysis support of various sections of power systems are studied to provide techno-economic benefits and moderate the operational cost of various levels of generation and distribution sectors[39, 40]. An overview of Performance enhancement parameters and reliability indices for various scenarios is given in Table 13.

Based on the studies of various scenarios in IEEE 33 bus RDN and IEEE 69 bus RDN, the following inferences are presented:

- The Mayfly Optimization Algorithm (MOA) is implemented to achieve the optimum allocation of distributed energy sources into RDN for both grid-connected and islanded modes. Supply and demand balance is maintained even in islanding conditions by interconnecting PV and WT units with STATCOM into IEEE-33 bus RDN and IEEE-69 bus RDN.
- The reliability assessment of IEEE - 33 bus RDN and IEEE - 69 bus RDN, which are integrated with DG sources for various scenarios, reveals the benefits of addressing uncertainties in load operations. It is clear that

reliability indices SAIFI and SAIDI in scenarios 3 and 4 of IEEE 33 bus RDN are reduced from 2.5894 f/c.yr to 2.5719 f/c.yr and 2.2990 hr/c. yr to 1.7114 hr/c.yr. Similarly, for the IEEE- 69 bus, the SAIFI of scenarios 3 and 4 are minimized from 1.8874 f/c. yr to 1.5959 f/c. yr and SAIDI of scenarios 1 and 2 are reduced from 1.2091 hr/c.yr to 1.2054 hr/c yr.

- It is observed that reliability indices ASAI in scenarios 3 and 4 of IEEE 33 bus have enhanced from 0.9997 p.u. to 0.9998 p.u. Similarly, in all the scenarios of IEEE 69 bus RDN from 0.9996 p.u. towards 0.9998 p.u. The reliability indices ASUI have reduced from 0.00026 p.u. to 0.00021 in scenarios 3 and 4 of IEEE 33 bus RDN. Thus, the reliability indices SAIDI, SAIFI, and ASAI mainly aid in mitigating future adverse effects in distribution networks.
- From the attained results, it is observed that IEEE- 33 bus and IEEE -69 bus RDN offer the efficiency of MOA through power loss reduction, upholding the good quality of voltage profile and reliability enhancement. When compared to the convergence characteristics of other existing algorithms like the Cuckoo Search Algorithm (CSA), Particle Swarm Optimization (PSO), Flower Pollination Algorithm (FPA), and Grasshopper Optimization Algorithm (GOA), MOA offers enhanced solution searching capabilities.
- Implementing network reconfiguration techniques lowers actual power losses and raises the power index of reliability, allowing power distribution operators to enhance the competence and reliability of the power distribution system.
- The Mayfly Optimisation Algorithm is a potent technology for improving power system performance, but

its ethical application necessitates thoughtful design decisions. To provide resilient, environmentally sustainable, and commercially competitive electric power systems, MOA-based solutions must integrate

sustainability, fairness, and accessibility. By addressing these issues, MOA helps to create power systems that are compatible with societal standards and long-term sustainability objectives.

**Table 13. Performance aspects and Reliability indices of IEEE -33 and IEEE -69 bus test systems under various scenarios**

<b>IEEE - 33 Bus test system</b>					
<b>Performance Aspects and reliability indices</b>	Base Case	Scenario 1	Scenario 2	Scenario 3	Scenario 4
<b>RES size and locations</b>	—	1090.97(24) 800.96(13) 1054.01(30)	1068.30/0.9(24) 789.30/0.9 (13) 1037.52/0.72(30)	882.03(30) 720.02(15) 967.51(3)	909.419/0.313(3) 837.090/0.882(8) 716.026/0.586(30)
<b>P<sub>loss</sub> (kW)</b>	210.99	72.787	11.749	56.440	25.128
<b>P IR</b>	0	0.7667	0.7787	0.6765	0.6561
<b>VDI</b>	0.0111	0.00373	0.0076	0.00302	0.00195
<b>V<sub>min</sub> (p.u.)</b>	0.9038	0.9687	0.9922	0.9694	0.9774
<b>SAIFI (f/c.yr)</b>	2.5894	2.5741	2.5741	2.5719	2.5719
<b>SAIDI (hr/c.yr)</b>	2.2990	2.2791	2.2791	1.7114	1.7114
<b>CAIDI (hr/c.int)</b>	0.8879	0.8854	0.8854	0.6654	0.6654
<b>ASAI (p.u.)</b>	0.9997	0.9997	0.9997	0.9998	0.9998
<b>ASUI (p.u.)</b>	0.00025	0.00026	0.00026	0.0002	0.0002
<b>IEEE - 69 Bus test system</b>					
<b>RES size and locations</b>	—	526.67(11) 380.539(17) 1718.98(61)	498.63/0.821(11) 376.25/0.828(18) 1686.92/0.823(61)	1403.42(49) 1334.64(61) 767.93(21)	1085.15/0.689(61) 1217.85/0.921(48) 494.29/0.780 (27)
<b>P<sub>loss</sub> (kW)</b>	225.007	150.974	96.130	38.403	14.246
<b>P IR</b>	0	0.691	0.674	0.912	0.732
<b>VDI</b>	0.0046	0.00105	0.00016	0.00183	0.00078
<b>V<sub>min</sub> (p.u.)</b>	0.9092	0.9790	0.9943	0.9728	0.9883
<b>SAIFI (f/c.yr)</b>	1.8874	1.8174	1.8174	1.5959	1.5959
<b>SAIDI (hr/c.yr)</b>	1.2091	1.2054	1.2054	1.2384	1.2384
<b>CAIDI (hr/c.int)</b>	0.6692	0.6638	0.6639	0.776	0.776
<b>ASAI (p.u.)</b>	0.9996	0.9998	0.9998	0.9998	0.9998
<b>ASUI (p.u.)</b>	0.00014	0.00012	0.00012	0.00012	0.00012

## 5. Conclusion

The Mayfly Optimization Algorithm (MOA), a recently created meta-heuristic algorithm with natural inspiration, is described in this research as a means of determining the accurate renewable energy-based distribution generation into distribution networks while also taking islanding mode and reconfiguration into account. Through the IEEE - 33 bus and IEEE - 69 bus systems, the suggested technique has been verified for four different scenarios, and the results are superior to other heuristic methods that have been employed in the literature. According to the study's findings, the MOA convergences fast when PV and WT are placed in the RDN optimally to lower voltage variation and reduce the overall power loss of the system. In addition, the proposed MOA reduced power losses by 56.44kW, 25.12kW, 38.40kW, and 14.24kW, respectively, while maintaining a minimum voltage of 0.9694(p.u.), 0.9779(p.u.), 0.9728(p.u.) and 0.9883(p.u.), which was better than the existing algorithms. As a result of improved radial distribution network performance, the power

index of reliability has increased to a maximum of 0.7787 and 0.9120. This type of study provides flexibility to power operators to address the challenges concerning integration issues of DG sources and power quality issues and to fulfill reliability objectives.

Due to the static nature and lack of adaptability of MOA, the optimisation process must be repeated with updated input data in the event of a malfunction or load discrepancy. It becomes challenging to deal with abrupt changes in the power system load. Future studies should concentrate on testing real-world distribution networks, incorporating multi-objective optimisation frameworks, and expanding MOA to dynamic and probabilistic scenarios. Its reliability perspective and its use in smart grid environments could be improved further by integrating MOA with other innovative techniques, such as dynamic optimization frameworks and reinforcement learning.

## Acknowledgments

S.B.A. and D.S. designed the problem under study; S.B.A conducted the simulations and produced the results, and D.S.

analyzed the results; S.B.A. prepared the paper, which D.S. further reviewed. All the authors have read and approved the published version of the manuscript.

## References

- [1] IRENA, *Global Renewables Outlook-Energy Transformation 2050*, International Renewable Energy Agency, 2020. [[CrossRef](#)] [[Google Scholar](#)] [[Publisher Link](#)]
- [2] K. Prakash et al., "Review of Power System Distribution Network Architecture," *2016 3<sup>rd</sup> Asia-Pacific World Congress on Computer Science and Engineering (APWC on CSE)*, Nadi, Fiji, pp. 124-130, 2016. [[CrossRef](#)] [[Google Scholar](#)] [[Publisher Link](#)]
- [3] Ezequiel Junio Lima, and Luiz Carlos Gomes Freitas, "Hosting Capacity Calculation Deploying a Hybrid Methodology: A Case Study Concerning the Intermittent Nature of Photovoltaic Distributed Generation and the Variable Nature of Energy Consumption in a Medium Voltage Distribution Network," *Energies*, vol. 15, no. 3, pp. 1-16, 2022. [[CrossRef](#)] [[Google Scholar](#)] [[Publisher Link](#)]
- [4] Shilpa Kalambe, and Ganga Agnihotri, "Loss Minimization Techniques used in Distribution Network: Bibliographical Survey," *Renewable and Sustainable Energy Reviews*, vol. 29, pp. 184-200, 2014. [[CrossRef](#)] [[Google Scholar](#)] [[Publisher Link](#)]
- [5] Mohamed A. Tolba et al., "Comprehensive Analysis of Optimal Allocation of Capacitor Banks in Various Distribution Networks using Different Hybrid Optimization Algorithms," *2017 IEEE International Conference on Environment and Electrical Engineering and 2017 IEEE Industrial and Commercial Power Systems Europe (EEEIC / I&CPS Europe)*, Milan, Italy, pp. 1-7, 2017. [[CrossRef](#)] [[Google Scholar](#)] [[Publisher Link](#)]
- [6] Varaprasad Janamala, and K. Radha Rani, "Optimal Allocation of Solar Photovoltaic Distributed Generation in Electrical Distribution Networks using Archimedes Optimization Algorithm," *Clean Energy*, vol. 6, no. 2, pp. 271-287, 2022. [[CrossRef](#)] [[Google Scholar](#)] [[Publisher Link](#)]
- [7] Mahsa Azarnia, Morteza Rahimiyan, and Pierluigi Siano, "Offering of Active Distribution Network in Real-Time Energy Market by Integrated Energy Management System and Volt-Var Optimization," *Applied Energy*, vol. 358, 2024. [[CrossRef](#)] [[Google Scholar](#)] [[Publisher Link](#)]
- [8] Hayfa Souifi, Omar Kahouli, and Hsan Hadj Abdallah, "Multi-Objective Distribution Network Reconfiguration Optimization Problem," *Electrical Engineering*, vol. 101, no. 1, pp. 45-55, 2019. [[CrossRef](#)] [[Google Scholar](#)] [[Publisher Link](#)]
- [9] Hossein Lotfi, Mohammad Ebrahim Hajiabadi, and Hossein Parsadust, "Power Distribution Network Reconfiguration Techniques: A Thorough Review," *Sustainability*, vol. 16, no. 23, pp. 1-33, 2024. [[CrossRef](#)] [[Google Scholar](#)] [[Publisher Link](#)]
- [10] Ali Ehsan, and Qiang Yang, "Optimal Integration and Planning of Renewable Distributed Generation in the Power Distribution Networks: A Review of Analytical Techniques," *Applied Energy*, vol. 210, pp. 44-59, 2018. [[CrossRef](#)] [[Google Scholar](#)] [[Publisher Link](#)]
- [11] Mahmoud Pesaran H.A, Phung Dang Huy, and Vigna K. Ramachandaramurthy, "Review of the Optimal Allocation of Distributed Generation: Objectives, Constraints, Methods, and Algorithms," *Renewable and Sustainable Energy Reviews*, vol. 75, pp. 293-312, 2017. [[CrossRef](#)] [[Google Scholar](#)] [[Publisher Link](#)]
- [12] Ali Selim et al., "Optimal Placement of DGs in Distribution System Using an Improved Harris Hawks Optimizer Based on Single- and Multi-Objective Approaches," *IEEE Access*, vol. 8, pp. 52815-52829, 2020. [[CrossRef](#)] [[Google Scholar](#)] [[Publisher Link](#)]
- [13] Ahmed S. Hassan et al., "Optimal Integration of Distributed Generation Resources in Active Distribution Networks for Techno-Economic Benefits," *Energy Reports*, vol. 6, pp. 3462-3471, 2020. [[CrossRef](#)] [[Google Scholar](#)] [[Publisher Link](#)]
- [14] Pushpendra Singh et al., "Multi-Criteria Decision-Making Monarch Butterfly Optimization for Optimal Distributed Energy Resources Mix in Distribution Networks," *Applied Energy*, vol. 278, 2020. [[CrossRef](#)] [[Google Scholar](#)] [[Publisher Link](#)]
- [15] Mahiraj Singh Rawat, and Shelly Vadhera, "Probabilistic Approach to Determine Penetration of Hybrid Renewable DGS in Distribution Network Based on Voltage Stability Index," *Arabian Journal for Science and Engineering*, vol. 45, pp. 1473-1498, 2020. [[CrossRef](#)] [[Google Scholar](#)] [[Publisher Link](#)]
- [16] Mahmoud G. Hemeida et al., "Distributed Generators Optimization Based on Multi-Objective Functions Using Manta Rays Foraging Optimization Algorithm (MRFO)," *Energies*, vol. 13, no. 15, pp. 1-24, 2020. [[CrossRef](#)] [[Google Scholar](#)] [[Publisher Link](#)]
- [17] Ali Selim et al., "Optimal Setting of PV and Battery Energy Storage in Radial Distribution Systems using Multi-Objective Criteria with Fuzzy Logic Decision-Making," *IET Generation, Transmission and Distribution*, vol. 15, no. 1, pp. 135-148, 2020. [[CrossRef](#)] [[Google Scholar](#)] [[Publisher Link](#)]
- [18] Rabea Jamil Mahfoud et al., "A Novel Combined Evolutionary Algorithm for Optimal Planning of Distributed Generators in Radial Distribution Systems," *Applied Science*, vol. 9, no. 16, pp. 1-32, 2019. [[CrossRef](#)] [[Google Scholar](#)] [[Publisher Link](#)]
- [19] Thandava Krishna Sai Pandiraju, and Varaprasad Janamala, "Butterfly Optimization Algorithm-Based Optimal Sizing and Integration of Photovoltaic System in Multi-lateral Distribution Network for Interoperability," *Lecture Notes in Networks and Systems*, pp. 201-209, 2021. [[CrossRef](#)] [[Google Scholar](#)] [[Publisher Link](#)]



- [20] D.B. Prakash, and C. Lakshminarayana, "Multiple DG Placements in Radial Distribution System for Multi Objectives Using Whale Optimization Algorithm," *Alexandria Engineering Journal*, vol. 57, no. 4, pp. 2797-2806, 2018. [[CrossRef](#)] [[Google Scholar](#)] [[Publisher Link](#)]
- [21] Ali Selim et al., "Optimal Allocation of Multiple Types of Distributed Generations in Radial Distribution Systems Using a Hybrid Technique," *Sustainability*, vol. 13, no. 12, pp. 1-31, 2021. [[CrossRef](#)] [[Google Scholar](#)] [[Publisher Link](#)]
- [22] M.R. Elkadeem et al., "Optimal Planning of Renewable Energy-Integrated Distribution System Considering Uncertainties," *IEEE Access*, vol. 7, pp. 164887-164907, 2019. [[CrossRef](#)] [[Google Scholar](#)] [[Publisher Link](#)]
- [23] Tri Phuoc Nguyen, and Dieu Ngoc Vo, "A Novel Stochastic Fractal Search Algorithm for Optimal Allocation of Distributed Generators in Radial Distribution Systems," *Applied Soft Computing*, vol. 70, pp. 773-796, 2018. [[CrossRef](#)] [[Google Scholar](#)] [[Publisher Link](#)]
- [24] Mohamed, Emad et al., "Genetic-Moth Swarm Algorithm for Optimal Placement and Capacity of Renewable DG Sources in Distribution Systems," *International Journal of Interactive Multimedia and Artificial Intelligence*, vol. 5, no. 7, pp. 105-117, 2019. [[CrossRef](#)] [[Google Scholar](#)] [[Publisher Link](#)]
- [25] Pushpendra Singh, S.K. Bishnoi, and Nand K. Meena, "Moth Search Optimization for Optimal DERs Integration in Conjunction to OLTC Tap Operations in Distribution Systems," *IEEE Systems Journal*, vol. 14, no. 1, pp. 880-888, 2020. [[CrossRef](#)] [[Google Scholar](#)] [[Publisher Link](#)]
- [26] Babak Jeddi et al., "Robust Optimization Framework for Dynamic Distributed Energy Resources Planning in Distribution Networks," *International Journal of Electrical Power and Energy Systems*, vol. 110, pp. 419-443, 2019. [[CrossRef](#)] [[Google Scholar](#)] [[Publisher Link](#)]
- [27] R. Srinivasa Rao et al., "Power Loss Minimization in Distribution System Using Network Reconfiguration in the Presence of Distributed Generation," *IEEE Transactions on Power Systems*, vol. 28, no. 1, pp. 317-325, 2013. [[CrossRef](#)] [[Google Scholar](#)] [[Publisher Link](#)]
- [28] B. Kiran Babu, and Sydulu Maheswarapu, "An Optimal Accommodation of Distributed Generation in Power Distribution Systems," *20<sup>th</sup> National Power Systems Conference*, Tiruchirappalli, India, pp. 1-6, 2018. [[CrossRef](#)] [[Google Scholar](#)] [[Publisher Link](#)]
- [29] Eyad S. Oda et al., "Distributed Generations Planning using Flower Pollination Algorithm for Enhancing Distribution System Voltage Stability," *Ain Shams Engineering Journal*, vol. 8, no. 4, pp. 593-603, 2017. [[CrossRef](#)] [[Google Scholar](#)] [[Publisher Link](#)]
- [30] Osama Aslam Ansari, Nima Safari, and C. Y. Chung, "Reliability Assessment of Microgrid with Renewable Generation and Prioritized Loads," *IEEE Green Energy and Systems Conference*, Long Beach, CA, USA, pp. 1-6, 2016. [[CrossRef](#)] [[Google Scholar](#)] [[Publisher Link](#)]
- [31] Vishalini Divakar, M.S. Raviprakash, and B.K. Keshavan, "A Survey on Methods of Evaluation of Reliability of Distribution Systems with Distributed Generation," *International Journal of Engineering Research and Technology*, vol. 5, no. 8, pp. 220-226, 2016. [[Google Scholar](#)] [[Publisher Link](#)]
- [32] Amin Abedi, Ludovic Gaudard, and Franco Romerio, "Review of Major Approaches to Analyze Vulnerability in Power System," *Reliability Engineering and System Safety*, vol. 183, pp. 153-172, 2019. [[CrossRef](#)] [[Google Scholar](#)] [[Publisher Link](#)]
- [33] Juan A. Martinez, and Jean Mahseredjian, "Load Flow Calculations in Distribution Systems with Distributed Resources. A Review," *IEEE Power and Energy Society General Meeting*, Detroit, MI, USA, pp. 1-8, 2011. [[CrossRef](#)] [[Google Scholar](#)] [[Publisher Link](#)]
- [34] Konstantinos Zervoudakis, and Stelios Tsafarakis, "A Mayfly Optimization Algorithm," *Computers and Industrial Engineering*, vol. 145, 2020. [[CrossRef](#)] [[Google Scholar](#)] [[Publisher Link](#)]
- [35] Giridhar et al., "Mayfly Algorithm for Optimal Integration of Hybrid Photovoltaic / Battery Energy Storage/D-STATCOM System for Islanding Operation," *International Journal of Intelligent Engineering and Systems*, vol. 15, no. 3, pp. 225-232, 2022. [[Google Scholar](#)] [[Publisher Link](#)]
- [36] Kirti Maheshwari, and Santosh Kumar, "33Bus System DG Size Location Optimization using Artificial Intelligence," *International Research Journal of Engineering and Technology*, vol. 7, no. 9, pp. 266-274, 2020. [[Google Scholar](#)] [[Publisher Link](#)]
- [37] Dhanasekaran Boopathi et al., "Frequency Regulation of Interlinked Microgrid System Using Mayfly Algorithm-Based PID Controller," *Sustainability*, vol. 15, no. 11, pp. 1-19, 2023. [[CrossRef](#)] [[Google Scholar](#)] [[Publisher Link](#)]
- [38] T. Yuvaraj, and K. Ravi, "Multi-Objective Simultaneous DG and DSTATCOM Allocation in Radial Distribution Networks Using Cuckoo Searching Algorithm," *Alexandria Engineering Journal*, vol. 57, no. 4, pp. 2729-2742, 2018. [[CrossRef](#)] [[Google Scholar](#)] [[Publisher Link](#)]
- [39] Attia El-Fergany, "Optimal Allocation of Multi-Type Distributed Generators using Backtracking Search Optimization Algorithm," *International Journal of Electrical Power and Energy Systems*, vol. 64, pp. 1197-1205, 2015. [[CrossRef](#)] [[Google Scholar](#)] [[Publisher Link](#)]
- [40] Mengling Zhao, Xinlu Yang, and Xinyu Yin, "An Improved Mayfly Algorithm and Its Application," *AIP Advances*, vol. 12, no. 10, 2022. [[CrossRef](#)] [[Google Scholar](#)] [[Publisher Link](#)]